JEE Journal of Ecological Engineering

Journal of Ecological Engineering, 2026, 27(11), 477–491
https://doi.org/10.12911/22998993/231510
ISSN 2299–8993, License CC-BY 4.0

Received: 2026.08.10
Accepted: 2026.09.15
Published: 2026.10.01

Pollution and ecological risk of the potentially toxic elements (arsenic, lead, and cadmium) in acid mine drainage-impacted waters of Lake Uru Uru and tributaries, a Ramsar site, Bolivia

Carolina Montes-Dávalos[1*], Edwin Salcedo[2], Marcelo Herrera-Laura[1], Misael Mamani[3], Mariel Fernández[3]

[1] Department of Environmental Engineering, Universidad Católica Boliviana "San Pablo", La Paz, Bolivia
[2] School of Electronic Engineering and Computer Science, Queen Mary University of London, United Kingdom
[3] Department of Mechatronics Engineering, Universidad Católica Boliviana "San Pablo", La Paz, Bolivia
* Corresponding author's e-mail: carolinamontesdavalos@gmail.com

ABSTRACT

Acid mine drainage (AMD), owing to its high content of potentially toxic elements (PTEs), impacts ecosystem health through the contamination of tributary rivers. This study evaluates the spatial and temporal distribution of arsenic (As), lead (Pb), and cadmium (Cd) in the surface waters and AMD of the Lake Uru Uru watershed, a Ramsar site within the Oruro mining district (Bolivia), and quantifies the associated pollution and ecological risk. A total of 27 surface-water samples were collected during the wet and dry seasons, and their concentrations along with basic water-quality parameters were examined. Results revealed that the three PTEs were highly elevated, with maximum concentrations of As 12.80 mg/L (wet season), Pb 37.80 mg/L at a site near the mine (dry season), and Cd 4.18 mg/L (dry season), all exceeding international safety thresholds. Principal component analysis (PCA) explained 70.3 % of the variance in the first two components (PC1 = 49.4 %, PC2 = 20.9 %), separating urban mining-impacted sites (CT-01, CR-01) from rural sites. The ecological risk index indicated 100 % of sites exhibited high to extremely high risk, with CT-01 and RH-02 (near the mine) most affected during the dry season.

Keywords: acid mine drainage, Ramsar site, potentially toxic elements, ecological risk.

INTRODUCTION

Acid mine drainage (AMD) poses a serious environmental problem associated with the extraction of mineral resources (Cánovas et al., 2018). Generated by the oxidation of sulfide minerals, it persists over time and exhibits low pH and high concentrations of dissolved potentially toxic elements (PTEs) (Jiao et al., 2023). It contaminates surface water bodies, groundwater, and soils, where these PTEs are then redistributed through ion exchange, adsorption, and co-precipitation (Bu et al., 2024). Documented cases in the U.S. and Europe alone exceed 21,500 km of impacted watercourses (Caraballo et al., 2011), a figure that likely represents a conservative baseline of the true global extent.

In Latin America, widespread mining along the Andean polymetallic belt makes AMD-related contamination a major regional concern (Di Marzio et al., 2019). In these areas, rivers, streams, and wetlands act as primary receptors of waste derived from open-pit mining, and its accumulation drives progressive ecological degradation (Sun et al., 2020). In mining-adjacent urban centers, AMD mixes with municipal sewage through open drainage channels (Spellman et al., 2024), generating complex pollutant matrices with severe environmental and public health implications. Downstream, Ramsar-designated wetlands are especially vulnerable, as their biodiversity and nutrient cycling functions are essential for the well-being of adjacent communities (Rodríguez-Saldaña et al., 2026). These dual pressures converge in Andean cities such as Oruro, Bolivia, where centuries of polymetallic mining continue to affect both urban and rural aquatic systems (Rosenberg and Stålhammar, 2010). Lake Uru Uru therefore constitutes a representative case of the broader challenge faced by Ramsar-designated wetlands downstream of active mining districts worldwide.

Among the suite of contaminants associated with AMD, lead (Pb), cadmium (Cd), and arsenic (As) pose the most significant toxicity risks, even at trace levels (Shetaia et al., 2023). Their persistence and bioaccumulation potential make them especially concerning in aquatic systems (Galasso et al., 2025). Lead bioaccumulates in aquatic organisms, inducing oxidative stress, neurotoxicity, and immune dysfunction that impair reproduction (Zhang et al., 2024). Cadmium, in turn, accumulates in gills, liver, and kidneys, causing genotoxic damage (Chen et al., 2021), whereas arsenic biomagnifies along aquatic food webs (Aslam et al., 2024). Furthermore, PTEs have already been detected in endemic birds that use Ramsar wetlands as feeding and breeding habitats (Rocha et al., 2021). In humans, chronic exposure to these PTEs correlates with nephrotoxicity, neurodevelopmental impairment, and carcinogenesis in populations residing near contaminated water bodies (Saravanan et al., 2024).

Despite their ecological importance, high Andean wetlands in Bolivia have received limited scientific attention and rank among the country's most vulnerable ecosystems. Lake Uru Uru and Lake Poopó form a hydrologically linked lacustrine complex within the Titicaca–Desaguadero–Poopó–Coipasa (TDPS) system (Pillco Zolá and Bengtsson, 2006). Both lakes are jointly designated as a Ramsar Wetland of International Importance (Site No. 1181), encompassing 967,607 ha at over 3600 m above sea level (a.s.l.) (Ministerio de Medio Ambiente y Agua, 2015). The system supports exceptional biodiversity within the Puna ecoregion, providing refuge for 76 bird species, including the three Andean flamingo species (Chilean, Andean, and James's flamingos) and other endemic and vulnerable taxa (Coca Ignacio et al., 2024). It also sustains indigenous communities such as the Quechua San Agustín de Puñaca Ayllu, whose livelihoods depend directly on these water resources (Goudsmit Lambertín, 2021). Despite this protected status, the system functions as a terminal sink for AMD, untreated urban wastewater (Fontúrbel et al., 2011), and mining waste, a situation compounded by limited regulatory enforcement (Zamora Echenique and Calvo Vaca, 2021), illegal land occupation (La Patria, 2025), and stormwater drainage from the city of Oruro (Contraloría General del Estado, 2025). Because Lake Uru Uru integrates AMD inputs from urban and rural mining sources under a strongly seasonal semi-arid hydrological regime, it constitutes a representative model system for understanding PTE mobilization dynamics common to other seasonally dry, high-altitude mining-affected watersheds.

Studies on PTE contamination in the Lake Uru Uru system remain limited (Tapia et al., 2012), particularly with respect to seasonal surface-water monitoring across urban drainage channels, tributary rivers, and downstream rural areas affected by AMD. This gap is important because PTE concentrations in semi-arid terminal basins can vary substantially between wet and dry periods (Banks et al., 2004), influencing dilution capacity, PTE mobility, exposure pathways, and ecological risk (Yao et al., 2014). Therefore, assessing this urban–rural gradient across different seasons is necessary to reveal patterns of mining-related contamination that generate distinct risks for both environments.

Accordingly, this study aimed to: (1) determine the concentrations and spatiotemporal distribution of As, Pb, and Cd in surface waters along the urban–rural mining gradient of Lake Uru Uru; (2) assess pollution levels using the single-factor pollution index (Pi) and the Nemerow multi-factor index (Pn); and (3) evaluate ecological risk using the potential ecological risk index. These findings address a critical monitoring gap for this Ramsar-designated wetland and provide a framework for assessing surface waters affected by AMD.

MATERIALS AND METHODS

Study area

This research, was conducted in the polymetallic mining-affected region of Oruro (17°58'S, 67°07'W), Bolivia, at an elevation of 3735 m above sea level (Fontúrbel et al., 2011). According to the 2024 Population and Housing Census, the city of Oruro has a population of 571,471 (approximately 5.02% of Bolivia's total population) (Instituto Nacional de Estadística [INE], 2024). The city records an annual precipitation of 400 mm, with 280 mm (70%) concentrated between December and April. During the dry season, spanning from May to October, monthly values fall below 5 mm (Ferrari et al., 2025). The city's proximity to multiple mining centers in both urban and rural zones represent a significant risk factor for PTE dispersal, primarily through untreated AMD discharged into open street canals and adjacent surface water bodies (Quaghebeur et al., 2019). These effluents ultimately drain into the Ramsar-designated wetland system of Lakes Poopó and Uru Uru (Zamora Echenique and Trujillo Lunario, 2016), which constitutes the terminal receptor of this contamination gradient. A total of nine sampling sites were established across this hydrological network; detailed descriptions are provided in Table 1.

Sample collection and analysis

Samples were collected during three campaigns conducted in April, July, and September 2025 at the designated sampling sites (Figure 1), covering both wet and dry seasons. Surface water sampling was conducted across nine sites along a gradient from the urban mining environment of Oruro, upstream of Lake Uru Uru, to the rural area downstream. During September (dry season), CT-01 showed low flow, sediment buildup, and elevated suspended solids due to limited dilution. Winchester bottles were used for sampling; these were decontaminated by immersion in 10% nitric acid (HNO_3), followed by rinsing with distilled water and drying prior to use. In the field, the containers were rinsed with the sample prior to collection. For each site and campaign, three separate 50 mL samples were collected, one for each target element (As, Pb, Cd), at a depth of 8–15 cm below the water surface and preserved with 1 mL of concentrated HNO_3. Additional in situ physicochemical parameters were also measured at each station, including pH (HANNA HI98107), electrical conductivity (EC), and total dissolved solids (TDS) (HANNA HI98312). All instruments were calibrated prior to each sampling campaign. The samples were transported under refrigerated conditions and stored at 4 °C until digestion and analysis. PTE concentrations were determined by flame atomic absorption spectrometry (FAAS) on a PerkinElmer AAnalyst 200 instrument at the accredited Analytical Service Laboratory of the Institute of Chemical Research, Universidad Mayor de San Andrés (IIQ-UMSA). Method detection limits were 1.0 mg/L for As and 0.1 mg/L for Cd; Pb concentrations exceeded the limit of quantification in all analyzed samples. Sample concentrations below the LOD were assigned values equal to one-half the LOD (Helsel, 2006) prior to statistical and index-based analyses. Although conventional FAAS has limited sensitivity for As at trace levels, the method was suitable for quantifying the severe AMD-related contamination observed in the mg/L range. The R software was used to treat the results for statistical analysis, including

Table 1. Coordinates and descriptions of the sampling locations

Site	Coordinates	Code	Description
Urban zone			
1	17°56'28.7'' S, 67°06'36.7'' W	CT-01	Urban and AMD-influenced; "Copajira" canal.
2	17°57'03.8'' S, 67°05'45.7'' W	CR-01	Urban and AMD-influenced; final section of Tangarete Norte canal.
3	18°02'23.5'' S, 67°05'14.1'' W	PTRLU-01	Urban, WWTP and AMD-influenced; upstream of Lake Uru Uru.
4	18°01'55.4'' S, 67°09'03.1'' W	PE-01	Urban-influenced site; Tajarita River inflow to Lake Uru Uru; receives domestic wastewater from Aurora urban collector.
Rural zone			
5	18°09'27.1'' S, 67°04'54.0'' W	BP-01	Pumpulaya Bay; Southern part of Lake Uru Uru.
6	18°09'56.5'' S, 67°04'59.7'' W	BP-02	Pumpulaya Bay; Southern part of Lake Uru Uru.
7	18°09'53.5'' S, 66°58'51.98'' W	RH-01	AMD tributary to downstream of Lake Uru Uru; Huanuni River.
8	18°09'39.3'' S, 66°59'53.6'' W	RH-02	AMD tributary downstream of Lake Uru Uru; Huanuni River.
9	18°21'41.6'' S, 67°02'50.3'' W	RD-01	AMD-influenced; Desaguadero River.

Note: AMD – acid mine drainage; WWTP – wastewater treatment plant.

Spearman rank correlation and principal component analysis (PCA), and the Figures 1, 2 were created with Python using the Matplotlib and Seaborn libraries.

Environmental risk assessment

Pollution index

To assess contamination by PTEs in surface waters, the single-factor pollution index (Pi) and the Nemerow index (Pn) were employed (Li et al., 2018). The former measures the contamination level of each individual PTE and is calculated as follows:

$$P_i = \frac{C_i}{B_i} \quad (1)$$

where: P_i is the pollution index of element i, C_i is its measured concentration (mg L^{-1}), and B_i is the reference standard for that element.

To ensure consistency across all indices used in this study, B_i was set to the maximum allowable values (MAV) defined under the Portuguese/European legal framework for water quality (Decree-Law No. 236/98) (0.05, 0.05, and 0.005 mg L^{-1} for As, Pb, and Cd, respectively), rather than WHO drinking-water guideline values (World Health Organization, 2022), which are markedly more conservative and would artificially saturate the upper classes of the ecological risk index (RI) in this context. These values were adopted in the absence of nationally enforced maximum permissible limits for the studied water body. Using a single MAV across Pi, Pn, MI, and RI avoids this artifact and enables direct comparison among indices.

The Nemerow index provides an integrated assessment of contamination by multiple PTEs, while giving greater weight to the pollutant with the highest individual pollution index. This approach, which is widely applied in environmental assessments (Chen et al., 2015), is defined as:

$$P_n = \sqrt{\frac{\max(P_i)^2 + ave(P_i)^2}{2}} \quad (2)$$

where: P_i is the individual index of element i, max(Pi) the maximum value among all P_i, and ave(Pi) their average.

The classification criteria for P_i and P_n are detailed in Equation 3.

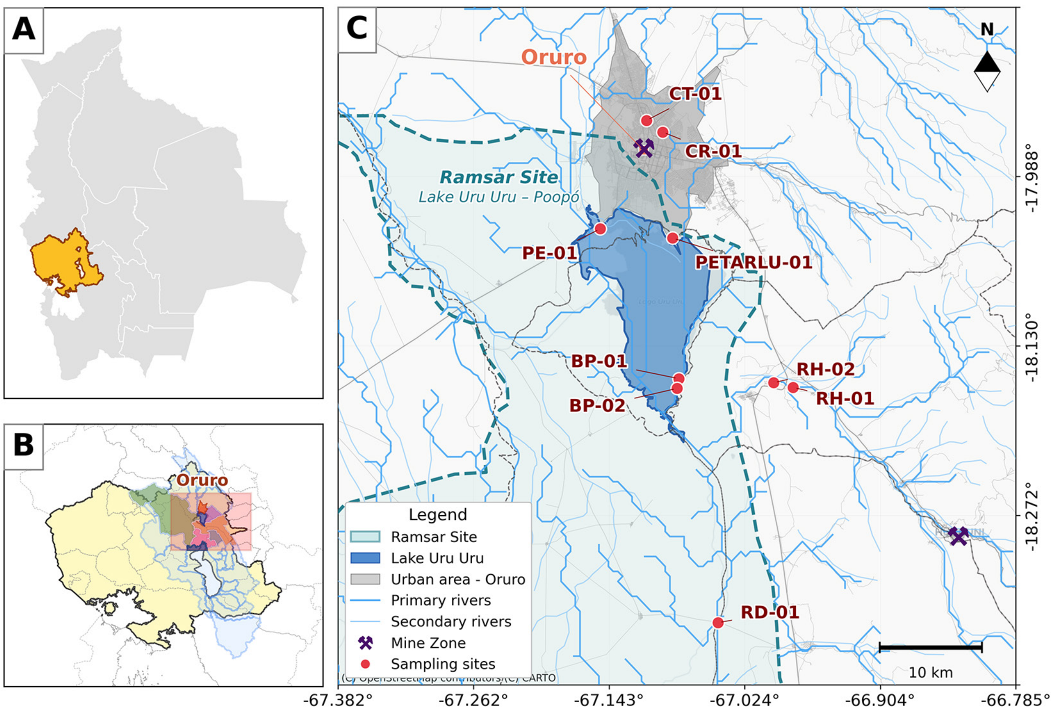

Figure 1. Location of the study area and monitoring points: (a) Oruro, Bolivia, (b) Poopó Basin and the Lake Uru Uru Ramsar Site in Oruro, (c) Location of sampling sites

Figure 2. Photographs of the sampling sites grouped into urban-influenced sites (top row) and rural sites (bottom row)

$$C(Pi) = \begin{cases} \textit{Unpolluted, } Pi < 1, \\ \textit{Slightly polluted, } 1 \le Pi < 2, \\ \textit{Moderately polluted, } 2 \le Pi < 3, \\ \textit{Highly polluted, } 3 \le Pi < 5, \\ \textit{Very highly polluted, } Pi \ge 5, \end{cases} \tag{3}$$

$$C(Pn) = \begin{cases} \textit{Safe, } Pn \le 0.7, \\ \textit{Precaution, } 0.7 < Pn \le 1, \\ \textit{Slight pollution, } 1 < Pn \le 2, \\ \textit{Moderate pollution, } 2 < Pn \le 3, \\ \textit{Heavy pollution, } Pn > 3. \end{cases}$$

Potential ecological risk

Potential ecological risk was assessed using the *potential ecological risk* index (RI) (Håkanson, 1980). The RI was calculated by summing the individual ecological risk factors (Eri) for the three PTEs:

$$RI = \sum_{i=1}^{3} E_r^i = \sum_{i=1}^{3} T_r^i \cdot C_f^i \tag{4}$$

where: the summation is performed over the three PTEs analyzed in this study (As, Pb, and Cd). T_r^i is the toxicity response coefficient of each element, as defined by Håkanson (1980) (As = 10, Pb = 5, Cd = 30), and C_f^i is the contamination factor, obtained by dividing the field-measured concentration (C_{sl}^i) by the reference value (MAV_i), such that $C_f^i = C_{sl}^i / MAV_n^i$.

The ecological risks associated with PTEs, based on RI values, were classified into four categories:
(I) RI < 150, slight ecological impact;
(II) 150 ≤ RI < 300, moderate ecological impact;
(III) 300 ≤ RI < 600, high ecological impact; and
(IV) RI ≥ 600, extremely high ecological consequences (Hakanson, 1980).

RESULTS AND DISCUSSION

Seasonal variability and water quality

Figure 3 summarizes the spatiotemporal variation of pH, electrical conductivity (EC), water temperature, and total dissolved solids (TDS) across the urban–rural sampling gradient during the three monitoring campaigns: April, July, and September. These parameters provide the hydrochemical context for interpreting PTE mobility and seasonal concentration patterns. Overall, the figure shows marked site-to-site contrasts and seasonal changes, distinguishing AMD-affected acidic waters with elevated ionic content from more neutral to alkaline waters in lacustrine and downstream areas.

Site CT-01, which directly receives AMD in the urban area, maintained an average pH of 1.81 ± 0.14 across the three campaigns, indicating severe acidification and consistent with the range previously reported for this channel (pH 1.2–2.5; Tapia et al., 2020). In contrast, PE-01, a peripheral site without direct AMD influence, showed pH values between 5.67 and 8.83. CR-01 and PTRLU-01 exhibited intermediate but more variable pH (2.43–6.15 and 4.80–6.93, respectively), with CR-01 becoming strongly acidic during the dry season (September). In the rural zone, RH-01 and RH-02, both AMD-affected tributary sites, also exhibited extremely acidic values, with pH ranging from 2.42–2.73 and 2.39–2.85, respectively. This likely reflects the long-term influence of the Huanuni tin (Sn) mining complex, which has operated for more than a century (Tapia et al., 2012). RD-01, located on the Desaguadero River, presented neutral to alkaline pH (6.40–8.26), whereas the most alkaline value was recorded at BP-02, a lacustrine sampling point in Lake Uru Uru, with a value of 10.23 in April. This alkaline extreme, also reflected at the adjacent BP-01 (pH 7.16–9.58), is consistent with an evaporative concentration effect previously documented for this area of the lake (station UU12), associated with the elevated salinity of these waters (Sarret et al., 2019).

Water temperature ranged from 12.0 °C to 26.9 °C, with the lowest values in July and the highest in September, particularly at the shallow lacustrine sites BP-01 and BP-02. The highest EC of the study was recorded at CT-01 in July (>20 mS/cm), saturating the multiparameter probe. At the same site, the September sample was analyzed by a certified external laboratory, which reported a TDS of 37.1 g/L; this extreme ionic load is attributable to the combination of untreated AMD, urban discharges, and low-flow conditions. Elevated values were also observed at PE-01 (8.66 g/L in July) and PTRLU-01 (9.50 g/L in September). In contrast, RH-01 presented the lowest TDS (0.62 g/L) in April, while RH-02 recorded the lowest EC (1.31 mS/cm) in the same period. Overall, EC and TDS followed the expected seasonal pattern of ionic concentration under low-flow conditions during the dry season and dilution during the wet season, most evident at the AMD-affected urban sites.

All measured PTE concentrations, together with the physicochemical parameters recorded at each site and campaign, are summarized in Table 2. The concentrations of As, Pb, and Cd exceeded the maximum allowable values (MAV) adopted in this study (0.05 mg/L for As and Pb; 0.005 mg/L for Cd) (Gomes and Valente, 2024) in all quantified samples and campaigns. At AMD-impacted sites, concentrations were markedly amplified during the dry season, likely driven by reduced dilution capacity and intensified evapoconcentration under Altiplano semi-arid conditions (Liu et al., 2022). Values below the detection limit for As and Cd were substituted with half the corresponding detection limit (Sojka and Jaskuła, 2022).

At CT-01 in the urban zone, Pb increased 51-fold between April (0.74 mg/L) and September (37.80 mg/L), while Cd increased 26-fold (0.16–4.18 mg/L). At CR-01, Pb rose 17.5-fold (0.81–14.20 mg/L) and Cd 20-fold (0.14–2.81 mg/L), consistent with the progressive transfer of the AMD signature from the urban source

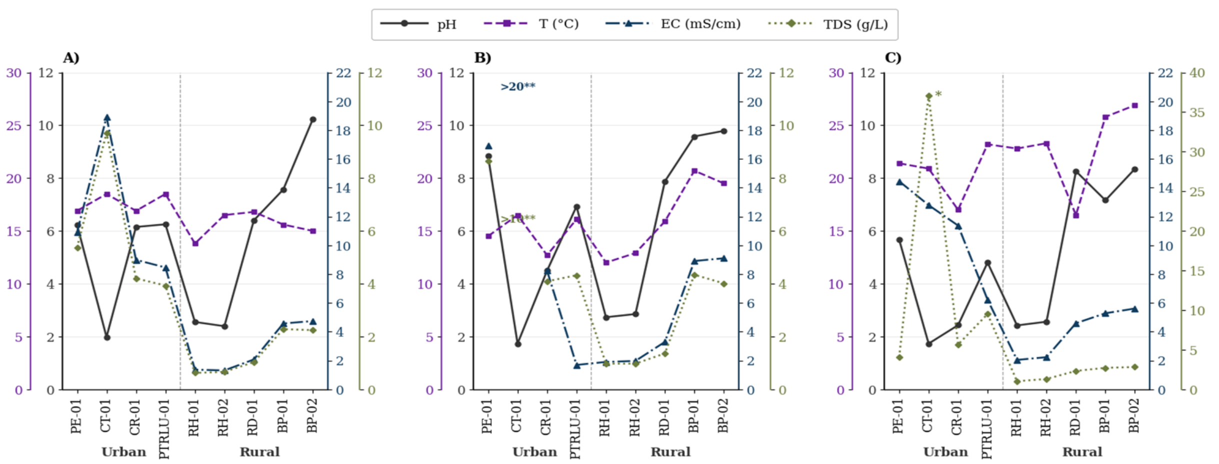

Figure 3. Physicochemical parameters (pH, EC, temperature, and TDS) in surface waters during: (a) the wet season, (b) the moderate-dry season, and (c) the dry season

Table 2. PTE concentrations and physicochemical parameters in surface water across the three sampling campaigns

Parameter	Month	CT-01	CR-01	PTRLU-01	PE-01	BP-01	BP-02	RH-01	RH-02	RD-01
As (mg/L)	Apr	<1	<1	1.44	<1	<1	10.80	6.80	12.80	<1
	Jul	<1	1.20	3.75	3.35	3.52	1.72	2.12	<1	3.05
	Sep	7.40	6.20	7.10	11.50	7.30	<1	7.50	2.90	8.70
Pb (mg/L)	Apr	0.74	0.81	0.75	0.69	0.67	0.95	0.98	22.10	0.76
	Jul	19.30	2.64	2.28	2.24	2.10	1.95	2.08	2.05	1.89
	Sep	37.80	14.20	5.78	3.20	3.80	3.30	2.20	3.60	5.98
Cd (mg/L)	Apr	0.16	0.14	<0.10	<0.10	<0.10	<0.10	0.19	0.23	<0.10
	Jul	2.54	0.56	0.36	0.12	0.14	0.10	0.94	1.52	0.11
	Sep	4.18	2.81	0.42	0.16	0.38	<0.10	2.02	1.62	0.11
T (°C)	Apr	18.5	16.9	18.5	16.9	15.6	15.0	13.8	16.5	16.8
	Jul	16.5	12.7	16.1	14.5	20.7	19.5	12.0	12.9	15.9
	Sep	20.9	17.0	23.2	21.4	25.8	26.9	22.8	23.3	16.5
pH	Apr	1.98	6.15	6.25	6.23	7.57	10.23	2.55	2.39	6.40
	Jul	1.73	4.49	6.93	8.83	9.58	9.79	2.73	2.85	7.88
	Sep	1.73	2.43	4.80	5.67	7.16	8.35	2.42	2.56	8.26
EC (mS/cm)	Apr	18.91	8.99	8.46	10.90	4.57	4.74	1.36	1.31	2.07
	Jul	>20.00**	8.24	1.69	16.92	8.91	9.10	1.90	1.97	3.29
	Sep	12.79	11.37	6.22	14.45	5.28	5.61	2.04	2.23	4.59
TDS (g/L)	Apr	9.71	4.20	3.93	5.37	2.28	2.24	0.62	0.66	1.03
	Jul	>10.00**	4.09	4.32	8.66	4.34	4.01	0.97	0.97	1.36
	Sep	37.10*	5.65	9.50	4.05	2.71	2.81	1.02	1.30	2.32

Note: Values below the limit of detection (LOD): As < 1 mg/L; Cd < 0.10 mg/L. For pollution and ecological-risk index calculations, values < LOD were substituted by half the LOD. * Value determined by certified external laboratory analysis. ** Value exceeds the instrument's measurement range.

toward the receiving channel as the dilution flow decreases (Romero et al., 2025). PE-01 recorded Pb (0.69–3.20 mg/L) and Cd (<0.10–0.16 mg/L) concentrations lower than at urban AMD sites but still above regulatory limits, indicating that even peripheral surface waters in Oruro present PTE contamination (Fontúrbel et al., 2011). The highest PTE concentrations were systematically recorded at CT-01, consistent with its proximity (~1 km) to the central urban mine.

In the rural zone, Pb, Cd, and As remained elevated across the three campaigns at the Huanuni River sites (RH-01 and RH-02), reflecting continuous AMD input (Aucour et al., 2026). During the wet season, RH-02 recorded the highest Pb and As concentrations among the sampled sites, with values of 22.10 mg/L and 12.80 mg/L, respectively. Downstream, the Desaguadero River (RD-01) reached As concentrations of 8.70 mg/L and Pb of 5.98 mg/L in September, a water body on which rural communities depend for irrigation and livestock. At Pumpulaya Bay (BP-01 and BP-02), As concentrations ranged from <1 mg/L to 10.80 mg/L, Pb from 0.67–3.80 mg/L, and Cd from <0.10 mg/L to 0.38 mg/L. Although lower than at direct AMD sites, these values still exceeded environmental quality limits. Consistently, sediment-focused studies in Lake Uru Uru have documented elevated As, Pb, Cd, and Sb concentrations (Tapia et al., 2012).

The overall distribution of PTE concentrations grouped by urban and rural zones across the three sampling campaigns is presented in Figure 4, illustrating the higher variability and elevated levels observed at urban sites, particularly for Pb and Cd during the dry season. Previous studies have reported for decades that AMD from mines enters tributary rivers and receiving water bodies (Anawar, 2013), altering the ecosystem due to its persistent and dispersive nature, with concentrations linked to the seasonality of precipitation. In Andean wetlands, such as the study area (Ramsar site), PTEs represent significant ecological risks (Bravo-Realpe et al., 2023), and the seasonal intensification of Pb and Cd observed here at AMD-impacted sites, driven by reduced dilution and dry-season evapoconcentration, mirrors patterns reported in other seasonally dry mining watersheds. In the semi-arid Puna of NW Argentina, AMD from the Pan de Azúcar mine, at a comparable elevation and connected to another Ramsar wetland, shows an analogous cycle: dry-season evaporation forms metal-rich salts later mobilized with the wet-season onset (Murray et al., 2021). Similar dry-season concentration maxima have been documented in the Tharsis mining district, Spain (Moreno González et al., 2020), and the associated "first flush" of acidity and metal load after the first rains has been reported in Mediterranean sulfide-mining districts (Caraballo et al., 2016).

Correlation analysis results

Statistically significant correlations among PTEs can indicate a common source or shared geochemical pathways (Luo et al., 2022). Spearman rank correlations were computed on site-level means ($n = 9$) across the three seasonal campaigns. The Spearman rank correlation matrix among PTEs (As, Cd, Pb) and physicochemical parameters (pH, temperature, EC, TDS) is shown in Figure 5. Cd and Pb exhibited a positive correlation ($\rho = 0.65$, $p = 0.058$), indicating a possible common source or similar geochemical behaviour. In contrast, pH and Cd showed a significant negative correlation ($\rho = -0.88$, $p < 0.01$). The lower the pH, the higher the content of Cd in the water, indicating that Cd in the water of the Lake Uru Uru tributaries is related to AMD. AMD increases the solubility of PTEs (Tapia et al., 2012), facilitating the release and transport of Cd^{2+} ions in surface waters. Pb showed a moderate negative trend with pH ($\rho = -0.43$), consistent with the expected dissolution of Pb under acidic conditions.

TDS and EC exhibited a strong and statistically significant positive correlation ($\rho = 0.88$, $p < 0.01$), which reflects the physicochemical coherence of the dissolved ionic load measurements. As concentrations did not show significant correlations with Cd, Pb, or pH, which suggests that As may originate from a different source than the polymetallic AMD inputs. This is possibly related to the natural geochemical background of As in the region, which has been reported as considerably elevated (Tapia et al., 2020).

Principal component analysis

Principal component analysis (PCA) was applied to the physicochemical parameters and PTE concentrations (pH, EC, TDS, As, Pb, and Cd) measured at each site-campaign observation ($n = 27$; nine sites × three seasonal campaigns), to explore the main multivariate gradients describing water-quality variability across the urban–rural sampling network; see Figure 6. All variables were standardized (zero mean, unit variance) prior to analysis. Non-detect values were substituted with one-half the limit of detection (As < 1 mg/L; Cd < 0.10 mg/L), and measurements exceeding the instrument's detection range (EC and TDS at CT-01 in July) were assigned the upper instrument limit (20.00 mS/cm and 10.00 g/L, respectively), consistent with Table 2. The first

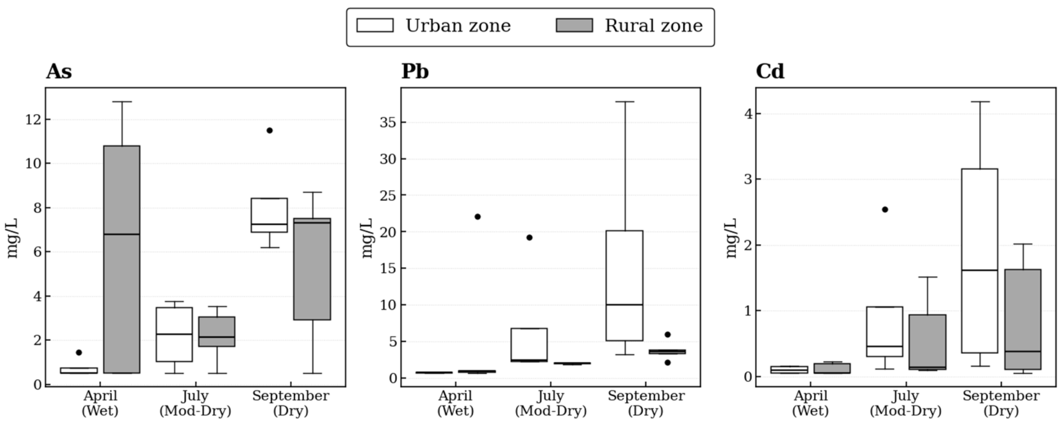

Figure 4. Box plots comparing As, Pb, and Cd concentrations (mg L^{-1}) between urban and rural zones across the three sampling campaigns (April: wet; July: moderate-dry; September: dry). Boxes indicate the interquartile range and median; whiskers extend to 1.5 × IQR, and points denote outliers. Pb and Cd were consistently higher in the urban zone, especially in September, while As showed the opposite pattern in April, converging between zones by September.

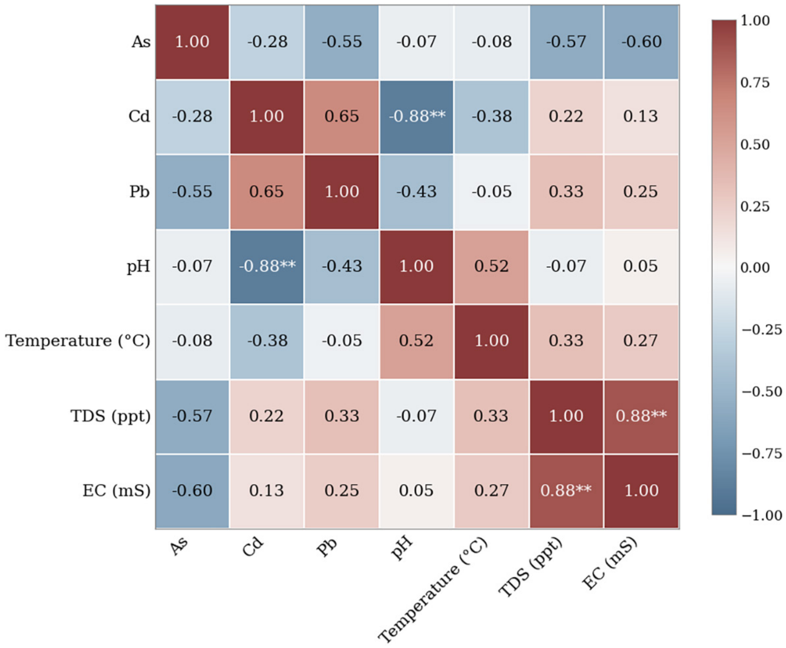

Figure 5. Spearman correlation matrix between PTE concentrations and physicochemical parameters in surface-water samples. Each cell shows the correlation coefficient (ρ), and asterisks indicate statistically significant correlations (**, $p < 0.01$)

two principal components explained 70.3% of the total variance, with PC1 accounting for 49.4% and PC2 for 20.9%. The PCA score plot shows that the most extreme AMD-affected samples, particularly CT-01 in July and September, were clearly separated from most other samples along PC1. Additional separation along PC2 was observed for some rural AMD-affected samples, especially RH-02 in April and RH-01 in September, indicating that both site-specific contamination intensity and seasonal conditions contributed to the observed hydrochemical variability. Overall, the PCA supports the visualization and distinction between highly impacted AMD samples and the remaining urban, lacustrine, and downstream waters. Excluding the censored CT-01 July observation from a sensitivity analysis changed the variance explained by PC1–PC2 only marginally (70.3% → 69.7%), with CT-01 remaining the most extreme AMD-impacted sample along PC1, confirming that this censoring does not affect the study's conclusions.

PTE POLLUTION ASSESSMENT

Figure 7 shows the results of the single-factor pollution index (Pi) and the Nemerow pollution index (Pn) for As, Pb, and Cd in the surface water samples from tributaries and Lake Uru Uru. For all sampling points, the Pi values for the assessed PTEs exceeded 5, corresponding to the "very highly polluted" category according to the adopted classification (Luo et al., 2022), indicating that the studied area is severely impacted by the assessed PTEs. The Pi values increased markedly from April to September at the urban AMD-impacted sites (CT-01, CR-01), with the Pi of Pb at CT-01 rising from 14.8 in April to 756.0 in September, and the Pi of Cd from 32.0 to 836.0 over the same period. At PE-01, a peripheral urban-influenced site, the highest Pi values appeared in September (As = 230.0).

At the rural AMD-impacted sites (RH-01, RH-02), the highest Pi values for Pb and As occurred in April (RH-02: Pi of Pb = 442.0; Pi of As = 256.0), while the highest Pi of Cd was observed in September (RH-01 = 404.0). At RD-01, downstream of the Huanuni AMD inputs, the Pi values increased gradually, peaking in September (As = 174.0; Pb = 119.6). At the lacustrine section (BP-01, BP-02), the Pi of As reached 216.0 at BP-02 in April. Overall, contamination levels are markedly elevated at all sites, posing a threat to these water bodies.

The Pn values exceeded 3 at all sampling points, indicating heavy pollution, with the most extreme values at the urban AMD-impacted sites

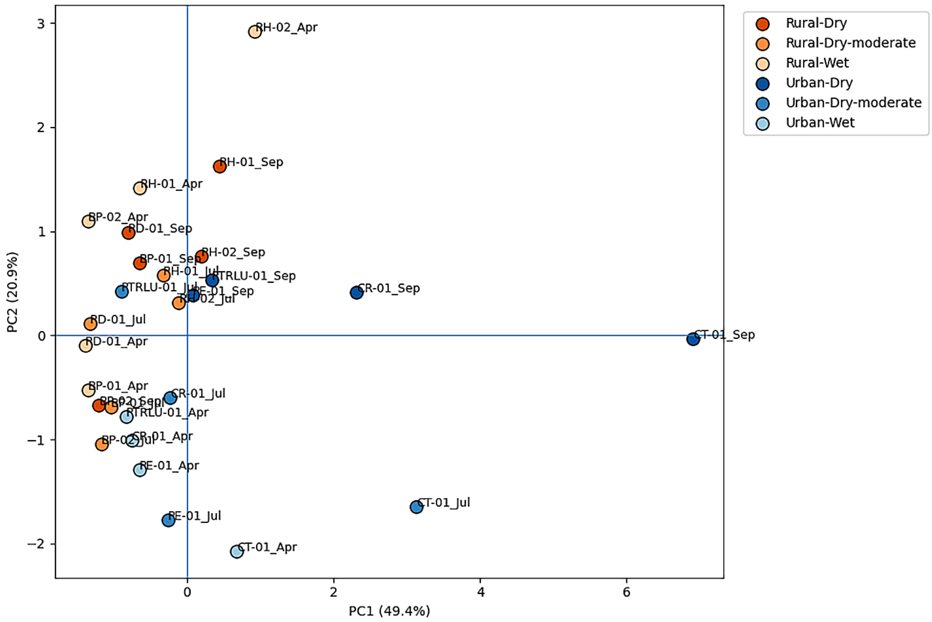

Figure 6. Principal component analysis (PCA) score plot based on standardized pH, EC, TDS, As, Pb, and Cd concentrations in surface-water samples. Points are colored according to sampling zone and hydrological season. Axis labels indicate the percentage of variance explained by each principal component

(CT-01, CR-01) and the rural AMD-impacted sites (RH-01, RH-02). This suggests that the urban AMD discharges have severely affected the upstream inflows of Lake Uru Uru (CT-01, CR-01, PE-01) and its lacustrine area (PTRLU-01, BP-01, BP-02), while the Huanuni AMD inputs have impacted the Desaguadero River (RD-01), underscoring AMD as the dominant driver of PTE contamination across the study area.

Comparable or even higher extreme values have been reported in AMD-impacted mining areas in China, with Pn values reaching up to 7673 (Jiao et al., 2023), as well as reported ranges of Pn = 0.90–407.49 (Xie and Ren, 2022), and Pn = 57 (Luo et al., 2022).

This indicates that such severe pollution observed in tributaries of Lake Uru Uru is consistent with patterns reported in other mining-affected aquatic systems.

Potential ecological risk

The potential ecological risk index, originally developed by Hakanson (1980) to quantify ecological risk from potentially toxic elements (PTEs) in sediments, has since been widely extended to other matrices, including surface water bodies (Banerjee et al., 2024; Dixit and Siddaiah, 2021; Hou et al., 2013; Mahmud et al., 2025). By combining PTE concentrations with their toxic-response coefficients, RI provides a single aggregated value reflecting the ecological risk of PTE contamination in aquatic systems (Azam and Tripathi, 2025). In the present study, this index was applied across wet, moderate-dry, and dry-season conditions, as these contrasting hydrological periods are known to influence dilution capacity, PTE mobility, and ecological exposure.

Table 3 presents the RI values and corresponding risk classifications for all sampling sites across the three hydrological seasons. No site exhibited low (RI < 150) or moderate (150 ≤ RI < 300) ecological risk at any point during the monitoring period.

In April (rainy season), PE-01, RD-01, and BP-01 showed high ecological risk (Class III), while CR-01, CT-01, PTRLU-01, BP-02, RH-01, and RH-02 were classified as Class IV (extremely high ecological consequences, RI ≥ 600). In July and September (moderate-dry and dry seasons), all nine sampling sites shifted into Class IV, indicating a widespread intensification of ecological risk as hydrological conditions transitioned toward the dry season. Based on their maximum RI values, the sampling sites followed the order: BP-02 < RD-01 < PE-01 < BP-01 < PTRLU-01 < RH-02 < RH-01 < CR-01 < CT-01, reflecting a consistent contamination gradient across the three sampling campaigns, with CT-01, CR-01, and RH-01, RH-02, consistently exhibiting the highest

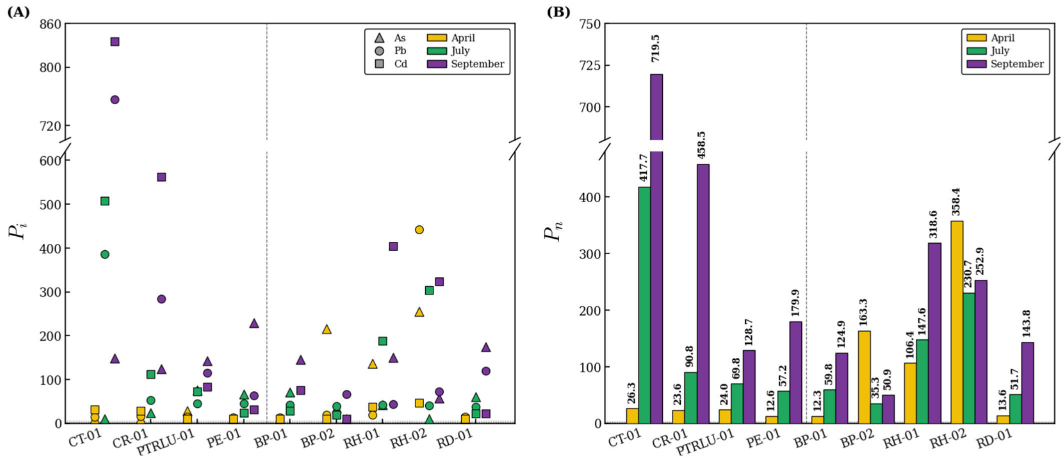

Figure 7. Single-factor pollution index (Pi) and Nemerow pollution index (Pn) for As, Pb, and Cd in surface waters of Lake Uru Uru and its tributaries across the three sampling campaigns

Table 3. Potential ecological risk index (RI) for sampled sites across three hydrological seasons. RI cells are shaded by risk class

Site	April		July		September	
	RI	Class	RI	Class	RI	Class
PE-01	4.69×10^2	III	1.61×10^3	IV	3.58×10^3	IV
CR-01	1.02×10^3	IV	3.86×10^3	IV	1.95×10^4	IV
CT-01	1.13×10^3	IV	1.73×10^4	IV	3.03×10^4	IV
PTRLU-01	6.63×10^2	IV	3.14×10^3	IV	4.52×10^3	IV
RD-01	4.76×10^2	III	1.46×10^3	IV	3.00×10^3	IV
BP-01	4.67×10^2	III	1.75×10^3	IV	4.12×10^3	IV
BP-02	2.56×10^3	IV	1.14×10^3	IV	7.30×10^2	IV
RH-01	2.60×10^3	IV	6.27×10^3	IV	1.38×10^4	IV
RH-02	6.15×10^3	IV	9.43×10^3	IV	1.07×10^4	IV

Note: Risk classes: I) RI < 150 (slight ecological impact); II) 150 ≤ RI < 300 (moderate ecological impact); III) 300 ≤ RI < 600 (high ecological impact); IV) RI ≥ 600 (extremely high ecological consequences).

values, particularly during the dry season. The extremely high ecological risk documented across the Lake Uru Uru watershed is consistent with values reported in other AMD-impacted surface waters worldwide. Direct AMD discharges in the Maramures mining region (Romania) were classified as very high to extremely strong risk, with RI values exceeding 5000 at several sites (Miclean et al., 2025). Similarly, a seasonal study of surface waters draining an abandoned sulfide mine in the Iberian Pyrite Belt (Portugal) reported ecological risk ranging from strong to extreme across a full hydrological year (Gomes and Valente, 2024), and comparably severe RI values have been documented in surface waters of an abandoned pyrite mining area in China (Jiao et al., 2023).

The presence of As, Pb, and Cd in surface waters poses a significant ecological risk due to their direct toxicity to aquatic organisms and other water-dependent biota, including livestock and endemic bird species (Osae et al., 2026). Consequently, this contamination represents a serious threat to both environmental and public health, particularly within a Ramsar-designated wetland ecosystem.

CONCLUSIONS

This study evaluated As, Pb, and Cd in surface waters and AMD of the Lake Uru Uru watershed across wet to dry seasons in regions of intensive mining activities. Most sites exceeded the adopted MAVs, with peak levels occurring at urban, AMD-impacted sites during the dry season, likely due to reduced dilution. A strong pH–Cd negative correlation and a Cd–Pb association suggest AMD mobilization, while As appears linked to the natural geochemical background in rural area. PCA separated urban mining-impacted from rural sites, consistent with the influence of mining-related and urban discharges. The ecological risk index classified most sites as high to extremely high risk, with CT-01, RH-01, and RH-02 particularly severe; these three sites remained in the extremely high category throughout the monitoring period. These results highlight the urgent need for AMD source control and continuous monitoring, plus targeted sediment studies at the most affected sites. Future monitoring should broaden the suite of analyzed PTEs beyond As, Pb, and Cd to include additional AMD-associated elements (e.g., Zn, Cu, Fe, Mn, Sb), enabling a more comprehensive characterization of contamination in the Lake Uru Uru system.

Acknowledgments

The research leading to the results presented here received funding from the Government of Canada through the Canadian Fund for Local Initiatives (CFLI 2024), Project No. CFLILIMA-BOL-0001.

REFERENCES

1. Anawar, H.M. (2013). Impact of climate change on acid mine drainage generation and contaminant transport in water ecosystems of semi-arid and arid mining areas. *Physics and Chemistry of the Earth, Parts A/B/C,* 58–60, 13–21. https://doi.org/10.1016/j.pce.2013.04.002
2. Aslam, H., Umar, A., Khan, M.U., Honey, S., Ullah, A., Ashraf, M.A. (2024). A review on heavy metals in ecosystems, their sources, roles, and impact on plant life. *Journal of Genetic Medicine and Gene Therapy*, *7*(1), 20–34. https://doi.org/10.29328/journal.jgmgt.1001012
3. Aucour, A.M., Sarret, G., Guédron, S., Tisserand, D., Duwig, C., Acha, D. (2026). Zn behavior and isotope fractionation in high altitude Andean lakes. *Environmental Pollution*, *399*, 128120. https://doi.org/10.1016/j.envpol.2026.128120
4. Azam, M.M., Tripathi, J.K. (2025). Health and ecological risk assessment of metals in surface water from the Himalayan tributaries of the Ganga River, India. *Geochemical Transactions, 26*, 3. https://doi.org/10.1186/s12932-025-00100-7
5. Banks, D., Markland, H., Smith, P.V., Mendez, C., Rodriguez, J., Huerta, A., Sæther, O.M. (2004). Distribution, salinity and pH dependence of elements in surface waters of the catchment areas of the Salars of Coipasa and Uyuni, Bolivian Altiplano. *Journal of Geochemical Exploration*, *84*(3), 141–166. https://doi.org/10.1016/j.gexplo.2004.07.001
6. Banerjee, T., Kumar, V., Sarkar, D.J., Roy, S., Jana, C., Behera, B.K., Das, B.K. (2024). Potentially toxic elements: distribution, ecological risk assessment and sources identification in a Himalayan lake in India. *Agricultural Res* 1–13. https://doi.org/10.1007/s40003-024-00720-y
7. Bravo-Realpe, I., Borja-Serrano, P., Rosero-Mayanquer, H., García-Garizabal, I., et al. (2023). Sedimentation rate and contamination levels profile of potentially toxic elements in the Limoncocha Lagoon RAMSAR wetland in the Ecuadorian Amazon. *Environments*, *10*(1), 2. https://doi.org/10.3390/environments10010002
8. Bu, C., Li, X., Li, Q., Li, L., Wu, P. (2024). Spatiotemporal distributions, sources, and health risks of heavy metals in an acid mine drainage (AMD)-contaminated karst river in southwest China. *Applied Water Science*, *14*(12), 251. https://doi.org/10.1007/s13201-024-02317-w
9. Cánovas, C.R., Riera, J., Carrero, S., Olías, M. (2018). Dissolved and particulate metal fluxes in an AMD-affected stream under different hydrological conditions: The Odiel River (SW Spain). *CATENA*, *165*, 414–424. https://doi.org/10.1016/j.catena.2018.02.020
10. Caraballo, M.A., Macías, F., Rötting, T.S., Nieto, J.M., Ayora, C. (2011). Long term remediation of highly polluted acid mine drainage: A sustainable approach to restore the environmental quality of the Odiel river basin. *Environmental Pollution*, *159*(12), 3613–3619. https://doi.org/10.1016/j.envpol.2011.08.003
11. Caraballo, M. A., Macías, F., Nieto, J. M., Ayora, C. (2016). Long term fluctuations of groundwater mine pollution in a sulfide mining district with dry Mediterranean climate: Implications for water resources management and remediation. *Science of the Total Environment, 539*, 427–435. https://doi.org/10.1016/j.scitotenv.2015.08.156
12. Chen, H., Teng, Y., Lu, S., Wang, Y., Wang, J. (2015). Contamination features and health risk of soil heavy metals in China. *Science of the Total Environment*, *512–513*, 143–153. https://doi.org/10.1016/j.scitotenv.2015.01.025
13. Chen, M., Ding, S., Li, C., Tang, Y., Fan, X., Xu, H., Tsang, D.C.W., Zhang, C. (2021). High cadmium pollution from sediments in a eutrophic lake. *Water Research*, *190*, 116711. https://doi.org/10.1016/j.watres.2020.116711

14. Coca Ignacio, F.E., Gutiérrez Miranda, A.J., Choque Escobar, K.F. (2024). La legislación boliviana ante la contaminación del Lago Uru Uru. *Ciencia Latina Revista Científica Multidisciplinar*, *8*(4), 7237–7255. https://doi.org/10.37811/cl_rcm.v8i4.13191 (in Spanish)
15. Contraloría General del Estado. (2025). *Boletín institucional*. https://www.contraloria.gob.bo (in Spanish)
16. Di Marzio, A., Lambertucci, S.A., Garcia Fernandez, A.J., Martínez-López, E. (2019). From Mexico to the Beagle Channel: A review of metal and metalloid pollution studies on wildlife species in Latin America. *Environmental Research*, *176*, 108462. https://doi.org/10.1016/j.envres.2019.04.029
17. Dixit, A., Siddaiah, N.S. (2021). Health and ecological risk assessment of metals in surface water from urban wetlands of Gurugram, India. *International Journal of Environmental Analytical Chemistry, 103*(19), 7606–7624. https://doi.org/10.1080/03067319.2021.1974012
18. Dong, J.-H., Bian, Z., Wang, H.-F. (2007). Comparison of heavy metal contents between different reclaimed soils and the control soil. *Journal of China University of Mining & Technology*, *36*, 531–536.
19. Ferrari, C., Resongles, E., Freydier, R., et al. (2025). Deciphering Sb sources and transport processes in a mining and smelting-impacted river system (Oruro, Bolivia): Insights from Sb isotopes. *Water, Air, & Soil Pollution*, *236*, 790. https://doi.org/10.1007/s11270-025-08445-6
20. Fontúrbel, F.E., Barbieri, E., Herbas, C., Barbieri, F.L., Gardon, J. (2011). Indoor metallic pollution related to mining activity in the Bolivian Altiplano. *Environmental Pollution*, *159*(10), 2870–2875. https://doi.org/10.1016/j.envpol.2011.04.039
21. Galasso, F., Frank, A.B., Foster, W.J. (2025). Heavy metal toxicity and its role as a major driver of past biodiversity crises. *Communications Earth & Environment*, *6*(1), 780. https://doi.org/10.1038/s43247-025-02781-5
22. Gomes, P., Valente, T. (2024). Seasonal impact of acid mine drainage on water quality and potential ecological risk in an old sulfide exploitation. *Environmental Science and Pollution Research*, *31*, 1–12. https://doi.org/10.1007/s11356-024-32367-1
23. Goudsmit Lambertín, A. (2021, May). San Agustín de Puñaca: minas abundantes y paisajes devastados. *Revista La Brava*. (in Spanish)
24. Hakanson, L. (1980). An ecological risk index for aquatic pollution control: A sedimentological approach. *Water Research*, *14*(8), 975–1001. https://doi.org/10.1016/0043-1354(80)90143-8
25. Hassan, M.R., Bhuiyan, M.N.H., Moniruzzaman, M., Mahmud, M.S., Samad, A. (2026). Pollution status and ecological risk assessment of heavy metals in surface water and sediment of an ecologically critical lake of Dhaka, Bangladesh. *Discover Water, 6*, 23. https://doi.org/10.1007/s43832-026-00346-x
26. Hou, D., He, J., Lü, C., Ren, L., Fan, Q., Wang, J., Xie, Z. (2013). Distribution characteristics and potential ecological risk assessment of heavy metals (Cu, Pb, Zn, Cd) in water and sediments from lake Dalinouer, China. *Ecotoxicology and Environmental Safety, 93*, 135–144. https://doi.org/10.1016/j.ecoenv.2013.03.012
27. Instituto Nacional de Estadística [INE]. (2024). *Censo de Población y Vivienda 2024 (CPV 2024)*. https://cpv2024.ine.gob.bo/ (in Spanish)
28. Jiao, B., Xu, G., Li, D., Yang, K., Luo, J. (2012). Hazards of heavy metals in coal. *Disaster Advances*, *5*(4), 1812–1818.
29. Jiao, Yanan, Zhang, C., Su, P., Tang, Y., Huang, Z., Ma, T. (2023). A review of acid mine drainage: Formation mechanism, treatment technology, typical engineering cases and resource utilization. *Process Safety and Environmental Protection*, *170*, 1240–1260. https://doi.org/10.1016/j.psep.2022.12.083
30. Jiao, Yiwen, Liu, Y., Wang, W., Li, Y., Chang, W., Zhou, A., Mu, R. (2023). Heavy metal distribution characteristics, water quality evaluation, and health risk evaluation of surface water in abandoned multi-year pyrite mine area. *Water*, *15*(17), 3138. https://doi.org/10.3390/w15173138
31. La Patria. (2025). *Construcciones ilegales afectan más de 400 hectáreas del Lago Uru Uru*. (in Spanish)
32. Li, L., Wu, J., Lu, J., Min, X., Xu, J., Yang, L. (2018). Distribution, pollution, bioaccumulation, and ecological risks of trace elements in soils of the northeastern Qinghai-Tibet Plateau. *Ecotoxicology and Environmental Safety*, *166*, 345–353. https://doi.org/10.1016/j.ecoenv.2018.09.110
33. Liu, Y., et al. (2022). Spatial distribution, source analysis and health risk study of heavy metals in the Liujiang River Basin in different seasons. *International Journal of Environmental Research and Public Health*, *19*(22), 15435. https://doi.org/10.3390/ijerph192215435
34. Luo, Y., Rao, J., Jia, Q. (2022). Heavy metal pollution and environmental risks in the water of Rongna River caused by natural AMD around Tiegelongnan copper deposit, Northern Tibet, China. *PLoS ONE*, *17*(4), e0266700. https://doi.org/10.1371/journal.pone.0266700
35. Mahmud, M.S., Rahman, M.S., Dina, S.A., Nasher, M.R., Choudhury, T.R., Begum, B.A., et al. (2025). Potential toxic elements in surface water of Mokosh Beel, Gazipur, Bangladesh: ecological and human health risk assessment for recreational users. *Heliyon.* https://doi.org/10.1016/j.heliyon.2025.e42421

36. Ministerio de Medio Ambiente y Agua. (2015). *Plan de acción para la conservación y el uso sustentable del Sitio Ramsar Lagos Poopó y Uru Uru, Oruro – Bolivia 2014–2023* [Technical report]. Viceministerio de Medio Ambiente, Biodiversidad, Cambios Climáticos y de Gestión y Desarrollo Forestal. (in Spanish)
37. Miclean, M., Cadar, O., Muntean, A., Levei, L. (2025). Mine water discharge chemistry and potential risk in a former mining area. *Environments, 12*(3), 76. https://doi.org/10.3390/environments12030076
38. Moreno González, R., Cánovas, C. R., Olías, M., Macías, F. (2020). Seasonal variability of extremely metal rich acid mine drainages from the Tharsis mines (SW Spain). *Environmental Pollution, 259*, 113829. https://doi.org/10.1016/j.envpol.2019.113829
39. Murray, J., Nordstrom, D. K., Dold, B., Kirschbaum, A. (2021). Seasonal fluctuations and geochemical modeling of acid mine drainage in the semi-arid Puna region: The Pan de Azúcar Pb–Ag–Zn mine, Argentina. *Journal of South American Earth Sciences, 109*, 103197. https://doi.org/10.1016/j.jsames.2021.103197
40. Osae, R., Hayford, O., Owusu, F., Aidoo, P. (2026). A literature review on heavy metal pollution in aquatic environments: Assessment methods, ecotoxicological impacts, and health risk implications. *Marine Pollution Bulletin*, *224*, 119045. https://doi.org/10.1016/j.marpolbul.2025.119045
41. Pillco Zolá, R., Bengtsson, L. (2006). Long-term and extreme water level variations of the shallow Lake Poopó, Bolivia. *Hydrological Sciences Journal*, *51*(1), 98–114. https://doi.org/10.1623/hysj.51.1.98
42. Quaghebeur, W., Mulhern, R.E., Ronsse, S., Heylen, S., Blommaert, H., Potemans, S., Valdivia Mendizábal, C., Terrazas García, J. (2019). Arsenic contamination in rainwater harvesting tanks around Lake Poopó in Oruro, Bolivia: An unrecognized health risk. *Science of the Total Environment*, *688*, 224–230. https://doi.org/10.1016/j.scitotenv.2019.06.126
43. Rocha, O., Pacheco, L.F., Ayala, G.R., Varela, F., Arengo, F. (2021). Trace metals and metalloids in Andean flamingos (*Phoenicoparrus andinus*) and Puna flamingos (*P. jamesi*) at two wetlands with different risk of exposure in the Bolivian Altiplano. *Environmental Monitoring and Assessment*, *193*(8), 535. https://doi.org/10.1007/s10661-021-09340-3
44. Rodríguez-Saldaña, V., Reyes-Gómez, V.M., Rodríguez-Maese, R., et al. (2026). Multivariate and index-based assessment of classical and emerging contaminants in Ramsar wetlands of northern Mexico. *Environmental Monitoring and Assessment*, *198*(4), 352. https://doi.org/10.1007/s10661-026-15199-z
45. Romero, A., González, I., Martín-Crespo, T., et al. (2025). Acid mine drainage and waste dispersion in legacy mining sites: An integrated approach using UAV photogrammetry and geospatial analysis. *Journal of Hazardous Materials*. https://doi.org/10.1016/j.jhazmat.2025.139445
46. Rosenberg, M., Stålhammar, K. (2010). *Evaluation of heavy metals in waters influenced by mining in the Poopó and Antequera River Basins, Oruro – Bolivia* [Master's thesis, Lund University]. Division of Water Resources Engineering.
47. Saravanan, A., Kumar, P.S., Ramesh, B., Srinivasan, S. (2024). Comprehensive review on toxic heavy metals in the aquatic system: Sources, identification, treatment strategies, and health risk assessment. *Environmental Research*, *258*, 119440. https://doi.org/10.1016/j.envres.2024.119440
48. Sarret, G., Guédron, S., Acha, D., et al. (2019). Extreme variability of arsenic bioaccumulation factor in Lake Titicaca, Bolivia. *Scientific Reports*, *9*, 10626. https://doi.org/10.1038/s41598-019-47183-8
49. Shetaia, S.A., Nasr, R.A., Lasheen, E.S.R., Dar, M.A., Al-Mur, B.A., Zakaly, H.M.H. (2023). Assessment of heavy metals contamination of sediments and surface waters of Bitter Lake, Suez Canal, Egypt. *Marine Pollution Bulletin*, *192*, 115096. https://doi.org/10.1016/j.marpolbul.2023.115096
50. Sojka, M., Jaskuła, J. (2022). Heavy metals in river sediments: Contamination, toxicity, and source identification—A case study from Poland. *International Journal of Environmental Research and Public Health*, *19*(17), 10502. https://doi.org/10.3390/ijerph191710502
51. Spellman, C.D., Burton, Z.T., Ikuma, K., Strosnider, W.H.J., Tasker, T.L., Roman, B., Goodwill, J.E. (2024). Continuous co-treatment of mine drainage with municipal wastewater. *Journal of Environmental Management*, *354*, 120282. https://doi.org/10.1016/j.jenvman.2024.120282
52. Sun, J., Strosnider, W.H.J., Nairn, R.W., LaBar, J.A. (2020). Water quality impacts of in-stream mine tailings on a headwater tributary of the Rio Pilcomayo, Potosí, Bolivia. *Applied Geochemistry*, *113*, 104464. https://doi.org/10.1016/j.apgeochem.2019.104464
53. Tapia, J., Audry, S., Townley, B., Duprey, J.L. (2012). Geochemical background, baseline and origin of contaminants from sediments in the mining-impacted Altiplano and Eastern Cordillera of Oruro, Bolivia. *Geochemistry: Exploration, Environment, Analysis*, *12*(1), 3–20. https://doi.org/10.1144/1467-7873/10-RA-049
54. Tapia, J., Audry, S., van Beek, P. (2020). Natural and anthropogenic controls on particulate metal(loid) deposition in Bolivian highland sediments, Lake Uru Uru (Bolivia). *The Holocene*, *30*(3), 473–488. https://doi.org/10.1177/0959683619887425

55. World Health Organization. (2022). *Guidelines for drinking-water quality: Fourth edition incorporating the first and second addenda*. World Health Organization.
56. Xiao, H., Shahab, A., Xi, B., Chang, Q., You, S., Li, J., Sun, X., Huang, H., Li, X. (2021). Heavy metal pollution, ecological risk, spatial distribution, and source identification in sediments of the Lijiang River, China. Environmental Pollution, 269, 116189. https://doi.org/10.1016/j.envpol.2020.116189
57. Xie, Q., Ren, B. (2022). Pollution and risk assessment of heavy metals in rivers in the antimony capital of Xikuangshan. *Scientific Reports*, *12*(1), 14393. https://doi.org/10.1038/s41598-022-18584-z
58. Yao, H., Qian, X., Gao, H., Wang, Y., & Xia, B. (2014). Seasonal and spatial variations of heavy metals in two typical Chinese rivers: Concentrations, environmental risks, and possible sources. *International Journal of Environmental Research and Public Health*, *11*(11), 11860–11878. https://doi.org/10.3390/ijerph111111860
59. Zamora Echenique, G., Calvo Vaca, J.A. (2021). Propuesta de rehabilitación ambiental del Lago Uru Uru. *Revista de Medio Ambiente y Minería*, *6*(1), 1–10. (in Spanish)
60. Zamora Echenique, G., Trujillo Lunario, E. (2016). Viabilidad del tratamiento de las aguas ácidas de la mina San José - Oruro – Bolivia. *Research, Society and Development*, *3*(2), 142–153. (in Spanish)
61. Zhang, H., Zhao, S., Shi, X., Sun, B., Cui, Z., Zhao, Y., Zhang, J. (2024). Distribution of characteristics, risk assessment, and source analysis of heavy metals in lake sediments. *Ecological Indicators*, *166*, 11234.